Effects of tidal periodicities and diurnal foraging constraints on the density of foraging wading birds

Authors: Calle, Leonardo, Gawlik, Dale E., Xie, Zhixiao, Green, Lauri, Lapointe, Brian, et al.

Source: The Auk, 133(3) : 378-396

Published By: American Ornithological Society

URL: https://doi.org/10.1642/AUK-15-234.1

The Auk
Ornithological Advances
AmericanOrnithology.org

Volume 133, 2016, pp. 378–396
DOI: 10.1642/AUK-15-234.1

RESEARCH ARTICLE

Effects of tidal periodicities and diurnal foraging constraints on the density of foraging wading birds

Leonardo Calle,[1,a]* Dale E. Gawlik,[1] Zhixiao Xie,[2] Lauri Green,[3] Brian Lapointe,[4] and Allan Strong[5]

[1] Environmental Science Program, Florida Atlantic University, Boca Raton, Florida, USA
[2] Department of Geosciences, Florida Atlantic University, Boca Raton, Florida, USA
[3] U.S. Environmental Protection Agency, Newport, Oregon, USA
[4] Harbor Branch Oceanographic Institute, Florida Atlantic University, Fort Pierce, Florida, USA
[5] The Rubenstein School of the Environment and Natural Resources, University of Vermont, Burlington, Vermont, USA
[a] Current address: Ecosystem Dynamics Laboratory, Department of Ecology, Montana State University, Bozeman, Montana, USA
* Corresponding author: leonardo.calle@msu.montana.edu

Submitted December 20, 2015; Accepted February 20, 2016; Published May 4, 2016

ABSTRACT

In intertidal zones, tidal cycles reduce water depths and provide areas of shallow water where wading birds can forage for aquatic prey (water depths 0–50 cm). However, a bird that forages diurnally can make use of only a portion of the tidal cycle, which can limit fulfillment of energetic demands. Furthermore, daily and biweekly (spring–neap) tides may compound effects on shallow-water availability for foraging birds. However, the relative effects of daily and biweekly tidal periodicities on the foraging ecology of wading birds are seldom investigated due to a lack of appropriate tools. Therefore, we developed a tidal simulation model to provide dynamic spatiotemporal estimates of the availability of water depths that are within the upper and lower bounds of the birds' foraging water depth limits ("shallow-water availability"). We studied two wading bird species, the Little Blue Heron (*Egretta caerulea*), a daytime-only forager, and the Great White Heron (*Ardea herodias occidentalis*), which feeds both diurnally and nocturnally, to evaluate the relative effects of daily and biweekly tides on shallow-water availability and on patterns in abundance of foraging birds. Seasonal foraging surveys ($n = 38$; 2011–2013) were conducted by boat along a 14-km transect adjacent to extensive intertidal flats in the lower Florida Keys, USA. For both species combined, biweekly tides resulted in a 0.61- to 6.09-fold change in abundance, whereas daily tides resulted in a 1.03- to 5.81-fold change in abundance. Diurnal shallow-water availability was not consistently correlated in magnitude or direction with spring–neap tidal cycles because differences in tide height between consecutive low tides were larger than changes in tidal amplitude from spring–neap tide cycles. Thus, the strong response by birds to the spring–neap tide was likely driven by mechanisms other than diurnal shallow-water availability alone.

Keywords: Egretta caerulea, foraging ecology, intertidal zone, moon phase, tidal model, tides, TiMSA, wading birds

Efecto de la periodicidad de la marea y de las restricciones alimentarias diurnas sobre la densidad de aves acuáticas que forrajean

RESUMEN

En las zonas intermareales, los ciclos de las mareas reducen la profundidad del agua y generan zonas de aguas someras donde las aves acuáticas pueden alimentarse de presas acuáticas (profundidad del agua entre 0–50 cm). Sin embargo, un ave que forrajea durante el día puede hacer uso solo de una parte del ciclo de la marea, lo que puede impedir que alcance sus requerimientos energéticos. Más aún, las mareas diarias y bi-semanales (marea muerta de primavera), pueden agravar los efectos en la disponibilidad de aguas someras para las aves forrajeras. Sin embargo, los efectos relativos de la periodicidad diaria y bi-semanal de las mareas en la ecología de forrajeo de las aves acuáticas son raramente investigados debido a la falta de herramientas apropiadas. Por ende, desarrollamos un modelo de simulación de mareas para brindar estimaciones espacio temporales dinámicas de la disponibilidad de aguas con profundidades dentro de los límites superior e inferior de los rangos de profundidad del agua para el forrajeo de las aves ("disponibilidad de aguas someras"). Estudiamos dos especies de aves acuáticas, *Egretta caerulea*, que forrajea solo de día, y *Ardea herodias occidentalis*, que se alimenta tanto de día como de noche, para evaluar los efectos relativos de las mareas diarias y bi-semanales en la disponibilidad de aguas someras y en los patrones de abundancia de las aves forrajeras. Los muestreos estacionales de forrajeo ($n = 38$; 2011–2013) fueron realizados en bote a lo largo de una transecta de 14 km adyacente a grandes bajos intermareales en los Cayos de Florida inferiores, USA. Para

ambas especies combinadas, las mareas bi-semanales produjeron un cambio de 0.61 a 6.09 veces en la abundancia, mientras que las mareas diarias produjeron un cambio de 1.03 a 5.81 veces en la abundancia. La disponibilidad de aguas someras diurnas no estuvo correlacionada consistentemente en magnitud o dirección con los ciclos de marea muerta de primavera debido a que las diferencias en la altura de la marea entre mareas bajas consecutivas fueron mayores que los cambios en la amplitud de la marea de los ciclos de la marea muerta de primavera. Por ende, la fuerte respuesta de las aves a la marea muerta de primavera fue probablemente impulsada por otros mecanismos distintos a la disponibilidad diurna de agua somera solamente.

Palabras clave: aves acuáticas, ecología de forrajeo, *Egretta caerulea*, fase lunar, mareas, modelo de mareas, zona intermareal, TiMSA

INTRODUCTION

In coastal areas, tidal dynamics support diverse aquatic and terrestrial species by regulating water levels and providing access to important intertidal habitats. These habitats are used for spawning, reproduction, refuge from predators, and foraging (Gibson 2003). The availability of intertidal zones may differ across species due to intrinsic physical limitations. For example, some short-legged wading birds require shallow water for foraging. Habitat availability may also be limited by behavioral constraints such as diurnal (Weisberg et al. 1981, Verwij et al. 2006, Santiago-Quesada et al. 2014), nocturnal (Dugan 1981, Sitters et al. 2001), or crepuscular feeding activity (Yu and Swennen 2004). Moreover, changes in the availability of intertidal habitat may impact species across trophic levels. For instance, some fishes may use intertidal zones as shallow-water refuges (Paterson et al. 2000, Gibson et al. 2002, Rieucau et al. 2015), whereas predatory wading birds may use intertidal zones as a primary habitat for feeding (Erwin 1996). In both examples, changes in the availability of intertidal habitat may affect a species' survival, energy budget, or pattern of abundance and distribution.

A first step toward assessing the effect of shallow-water availability on individuals or populations is to evaluate how shallow-water availability changes as a function of tidal dynamics. For wading birds in coastal areas, tides largely determine the availability of water depths that are within the upper and lower bounds of a bird's foraging limits, which generally are water depths of 0–50 cm ("shallow water"), depending on species. Although tides are not constant over time, tidal patterns can be successfully modeled by cyclic functions with harmonic periodicity at daily and biweekly (spring and neap tides) timescales (Cartwright and Melchior 1999). A spatiotemporal model of tides can help quantify the response of wading birds to tide-driven changes in shallow-water availability, which may provide insights to how populations are likely to respond to natural and anthropogenic changes in the availability of their foraging habitat.

In addition to physical factors that affect foraging habitat availability, species may have behavioral constraints that limit access to foraging habitat. Wading birds such as Little Blue Herons (*Egretta caerulea*) are diurnal visual hunters that may miss foraging opportunities that occur at night (Powell 1987, Rodgers and Smith 2012). Such behavioral constraints may limit access to foraging habitat for some species but not others (Kronfeld-Schor et al. 2003). For example, Great White Herons (*Ardea herodias occidentalis*) forage both diurnally and nocturnally (Vennesland and Butler 2011) thus can take advantage of all shallow-water foraging opportunities.

The interaction between time constraints on foraging (e.g., daytime-only feeding) and the tidal pattern adds complexity because these interactions can result in strong association, or disassociation, between abundance patterns and tidal periodicities at different timescales (Reise 1985; Figure 1). Moreover, the effects of tidal periodicities on species' abundance have seldom been investigated in wading birds (but see Matsunaga 2000). Analyses of tidal

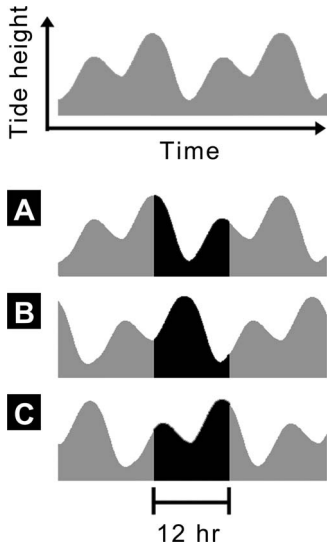

FIGURE 1. (Top) A mixed semi-diurnal tide (grey) results in 2 low tides per 24-hour period, each of unequal tide height, which differentially impacts shallow-water availability. The tidal signature (grey) shifts about 1 hr daily, resulting in daily (A–C), daytime (black, 12-hr) differences in low tide height. Time-shifts in the tidal pattern are more likely to affect daytime-only foragers such as the Little Blue Heron. By contrast, time-shifts in the tidal pattern should not affect species, such as the Great White Heron, that have the behavioral flexibility to access low tides during the day and night.

patterns and daytime feeding constraints may provide additional insight into the susceptibility of other time-constrained species to reductions in access to shallow-water habitat, such as may occur with sea level rise (Rozas 1995) and coastal development.

We evaluated the relative effects of 2 tidal periodicities, daily and biweekly cycles, on shallow-water availability and on the numerical response of wading birds foraging across ~830 ha of intertidal zone in the lower Florida Keys, USA. Our main hypotheses were that (I) shallow-water availability and biweekly tidal cycles (i.e. spring–neap tides) would be strongly correlated (positive for spring-tides and negative for neap-tides) only when no time constraint existed (that is, when birds can forage in the day and night) because the tide phase-shift would preclude such relationships from occurring during the daytime; (II) for both study species, increases in daily shallow-water availability would have a positive effect on bird abundance, because changes in daily, tide-driven, shallow-water availability would regulate foraging area for birds; (III) spring tides would have a positive effect on the abundance of foraging Great White Heron, and neap tides would have a negative effect, because biweekly changes in the tidal amplitude would increase shallow-water availability on top of daily tide-driven dynamics and day and night feeders would have greater access than time-constrained feeders; (IV) the abundance of foraging Little Blue Herons would be greatest when the low tide was early in the day because they do not feed at night and satiation may reduce their numbers at feeding areas later in the day; (V) the time of low tide would not be a significant factor for predicting the abundance of foraging Great White Herons because they have access to tides that occur both in the day and at night, as an effect of the time of the tide would only be important to time-constrained foragers.

METHODS

Study Area

The study area was within the boundaries of the Great White Heron National Wildlife Refuge (hereafter, Refuge) in the lower Florida Keys, Monroe County, Florida, USA (Figure 2). The Refuge experiences a mixed semidiurnal tide, which is "a tidal cycle with a high and low sea-level twice a day, with one of the two high tides being higher than the other high tide and one of the two low tides being lower than the other low tide" (Gill and Schultz 2001) (Figure 1). A mixed semidiurnal tide may have a large impact on shallow-water availability for Little Blue Herons that feed diurnally because periods of sufficiently low water may only occur once during a daytime low tide. During the study, low tides ranged from –0.15 to 0.20 m relative to the vertical datum Mean Lower Low Water (MLLW). Dominant habitats in the Refuge were 3,100 ha of mangrove islands surrounded by, and interspersed with, vast mud, sand, hard-bottom and seagrass flats. The mangrove islands serve as nesting sites for wading birds, whereas the tidal flats provide the majority of feeding habitat.

Study Species

Two wading bird species, the Little Blue Heron and the Great White Heron, provide a contrast of physical limitations (leg lengths) and behavioral constraints (diurnal or nocturnal activity, respectively) on foraging that allow us to evaluate the relative effects of daily and biweekly tidal cycles on shallow-water availability and on the abundance of foraging birds. Shallow water was defined as the range of water depths usable by each species, with the lower limit being zero, and the upper water depth limit bounded by the species' average leg length (Little Blue Heron = 22 cm, Great White Heron = 40 cm). Little Blue Herons generally left the roost at dawn and abandoned foraging at dusk even when shallow water was available (L. Calle and D. E. Gawlik, personal observation), which supports previous findings of day-only feeding habits (Powell 1987). In contrast, Great White Herons did not generally abandon foraging at dusk when shallow water was available (L. Calle and D. E. Gawlik, personal observation). Previous nighttime surveys of foraging Great Blue Herons (*Ardea herodias*) indicate that nighttime foraging does occur (Black and Collopy 1982, Powell 1987), but we could not quantify this effort because surveys were limited to the daytime.

Wading Bird Foraging Surveys

Wading bird foraging surveys ($n = 38$) were conducted seasonally from 2010 to 2013 to control for dispersal outside of the region, which may affect seasonal abundance (Melvin et al. 1999) (winter: $n = 7$; spring: $n = 11$; summer: $n = 14$; fall: $n = 6$). Surveys were conducted during the day by boat, at or near low tide, along a deep channel that forms the edge of extensive intertidal flats that extend from just southwest of Howe Key to Upper Harbor Key in the Refuge (Figure 2). At the start of each season, the direction of the survey was selected randomly and alternated on each subsequent survey. During surveys, the boat was stopped at intervals, ~500 m, which allowed for complete visual coverage of the transect by two observers using 10 × 42 or 10 × 50 binoculars; the spatial coordinates of each stop were recorded using a handheld global positioning systems unit (GPS 76; Garmin International, Olathe, Kansas, USA). At each stop, both surveyors visually searched one side of the survey transect for foraging wading birds; no attempt was made to survey the interior of mangrove islands. Birds in flight or perched in trees were not associated with foraging habitat and were

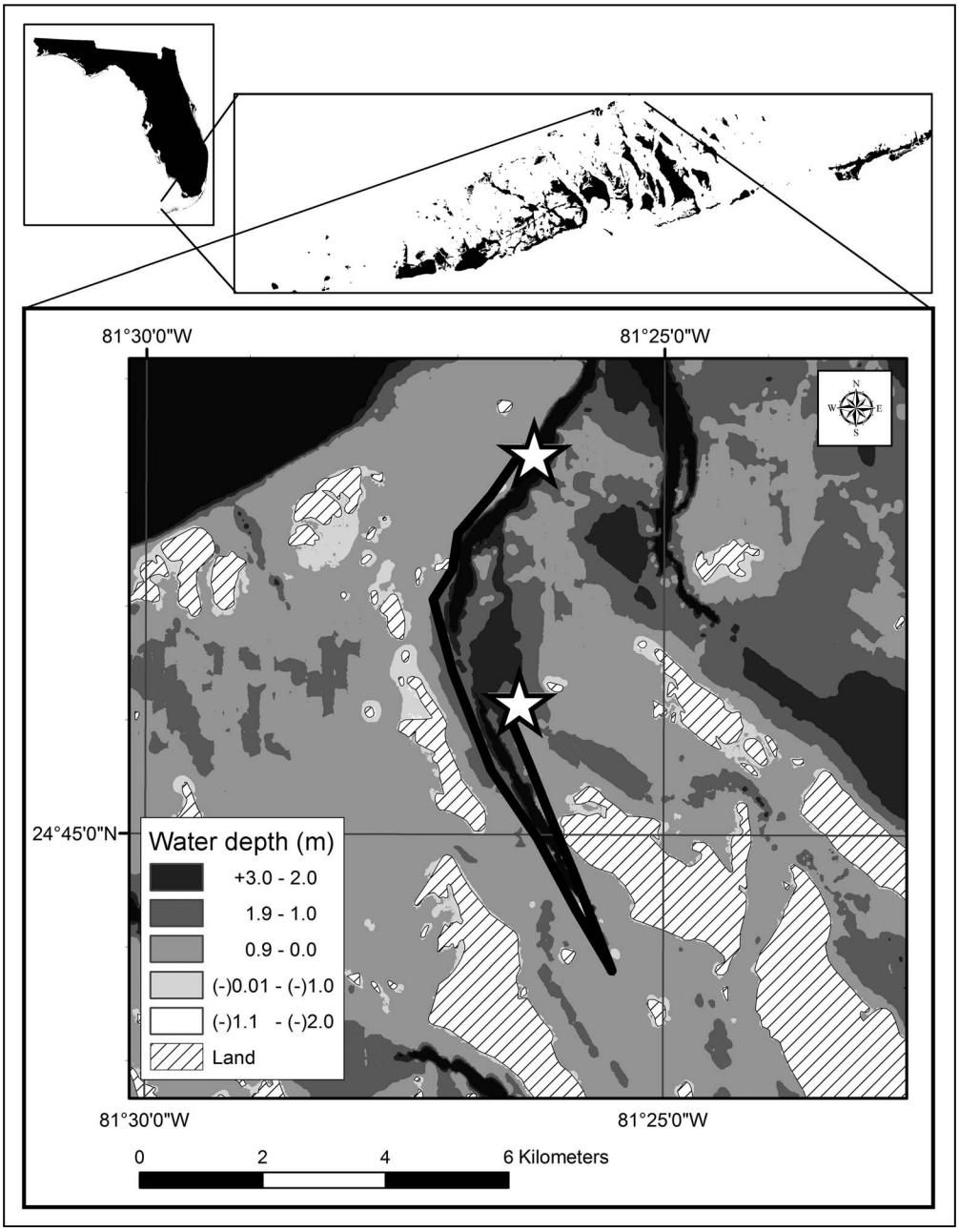

FIGURE 2. Route of distribution surveys (starred transect) within the study area overlaid on to a map of mean lower low water (MLLW).

therefore not counted. In 6 of 38 surveys, severe weather or lack of daylight precluded a complete survey of the study area. During the analysis, we controlled for the incomplete spatial coverage and variable survey duration by including a covariate for area of habitat surveyed and duration of the survey. Using the double-observer method (Nichols et al. 2000), we found that the detectability of wading birds foraging on tidal flats was close to one hundred percent up to 600 m from the transect. This was due to the lack of visible obstructions and conspicuous profiles of the birds. There was evidence of observer bias due to expertise, whereby novices (<1 yr birding experience) were more likely to confuse Tricolored Herons (*Egretta tricolor*) and Little Blue Herons. To minimize this bias, 1 of the 2 observers on each survey was experienced (>1 yr birding experience).

TABLE 1. Datasets have been compiled from freely available sources (USA). Data was compiled for 2011 and only for tide gauges that were inside the study area.

Dataset	Source	Hyperlink
Mean-Lower-Low-Water (MLLW) spatially explicit map	National Geophysical Data Center (NGDC)	http://www.ngdc.noaa.gov/mgg/coastal/coastal.html
Tidal Height, Time at Low/High Tide	National Oceanographic and Atmospheric Administration (NOAA)	http://co-ops.nos.noaa.gov/tide_predictions.html
Sunset/Sunrise Times	United States Naval Observatory (USNO)	http://aa.usno.navy.mil/data/

Description of Variables

Five variables known to affect the abundance of foraging wading birds were identified a priori through a literature review:

Survey start time relative to the time of sunrise (TimeFromSunrise). TimeFromSunrise was an integer variable on an interval scale. It was calculated as the difference between the time at the start of the survey and the time of sunrise, in minutes; the TimeFromSunrise across all surveys ranged from 46 to 792 min after sunrise. At the landscape scale, foraging locations were hypothesized to be selected by birds as the locations became available during the day. This was expected to affect the diurnally foraging Little Blue Heron and, in contrast, was not expected to be an important predictive variable for the diurnal/nocturnal foraging Great White Heron.

Survey start time relative to the time of low tide (TimeFromLowTide). TimeFromLowTide was an integer variable on an interval scale. It was calculated as the difference between the time at the start of the survey and the time at slack low tide, as determined by the nearest tidal gauge to the start location. Tidal gauge data were freely available from the National Oceanographic and Atmospheric Administration (NOAA; Table 1).

Personal observations (L. Calle and D. E. Gawlik) suggested that both of the heron species arrived at foraging locations on the ebbing tide as the locations became available, peaking in abundance before or during low tide, and staying at foraging locations until water depths were too deep for foraging. A similar association between water depth and the abundance of foraging birds has been found in freshwater (Gawlik 2002) and tidal wetlands (Matsunaga 2000, Dias et al. 2006, Raposa et al. 2009). Therefore, we expected to observe a greater abundance of foraging birds if surveys were started on the ebbing tide and continued through low tide, when foraging conditions were improving, than if surveys were started later on the flooding tide and continued as foraging conditions declined. Survey start times ranged from 220 min before to 70 min after low tide and continued for an average of 138 $\pm$ 35 min. It was not initially clear to us whether the patterns in abundance we were observing were due to ebb or flood tidal-flow preferences. We reasoned that the inclusion of the variable TimeFromLowTide in our analysis would provide such information, which would not be fully captured by the tidal model.

The Tidal Model used to estimate Shallow-water Availability. Shallow-water Availability was a continuous variable on a ratio scale. Our methods utilized a combined spatial–temporal estimate of shallow-water availability (units of hectare-hours) because daily tidal fluctuations affect the availability of water depths that are within a bird's foraging limits, both in space and time, but temporal constraints may be as important as spatial limitations. The tidal model, described as follows, estimated shallow-water availability independently for each species and for the duration of each survey.

We developed a Tidal Model of Shallow-water Availability (TiMSA) to provide spatiotemporal estimates of shallow-water availability for wading birds foraging at intertidal zones. The TiMSA utilizes freely available point-data for the height and time at high- and low-tide obtained from tidal gauges ($n = 3$) within the study area. The TiMSA simulates tides within individual polygons whose boundaries define an area that is closest to each data point, relative to all other data points in the model (i.e. Theissen, or Voronoi, polygons). Our polygon-based tidal model employed a data-assimilation approach where we applied a sinusoidal curve-fitting method to the point-data to simulate the rise and fall of water levels during tides and estimate water surfaces within each polygon. Water depths were estimated as the difference between the elevation of the predicted water level surface and the elevation of the benthic surface, obtained from a seamless benthic Digital Elevation Model (DEM) developed as part of the NOAA Tsunami Inundation Project. The DEM is a model developed from hydrographic survey soundings and multi-beam swath sonar surveys, with horizontal resolution of 30 m and an estimated vertical accuracy of 0.10 m in shallow waters or 5% of water depths in deeper waters (Grothe et al. 2011). We used the estimated water depths from TiMSA to calculate, for each species, the amount of time a particular location would have water depths within the range of usable water depths available for foraging

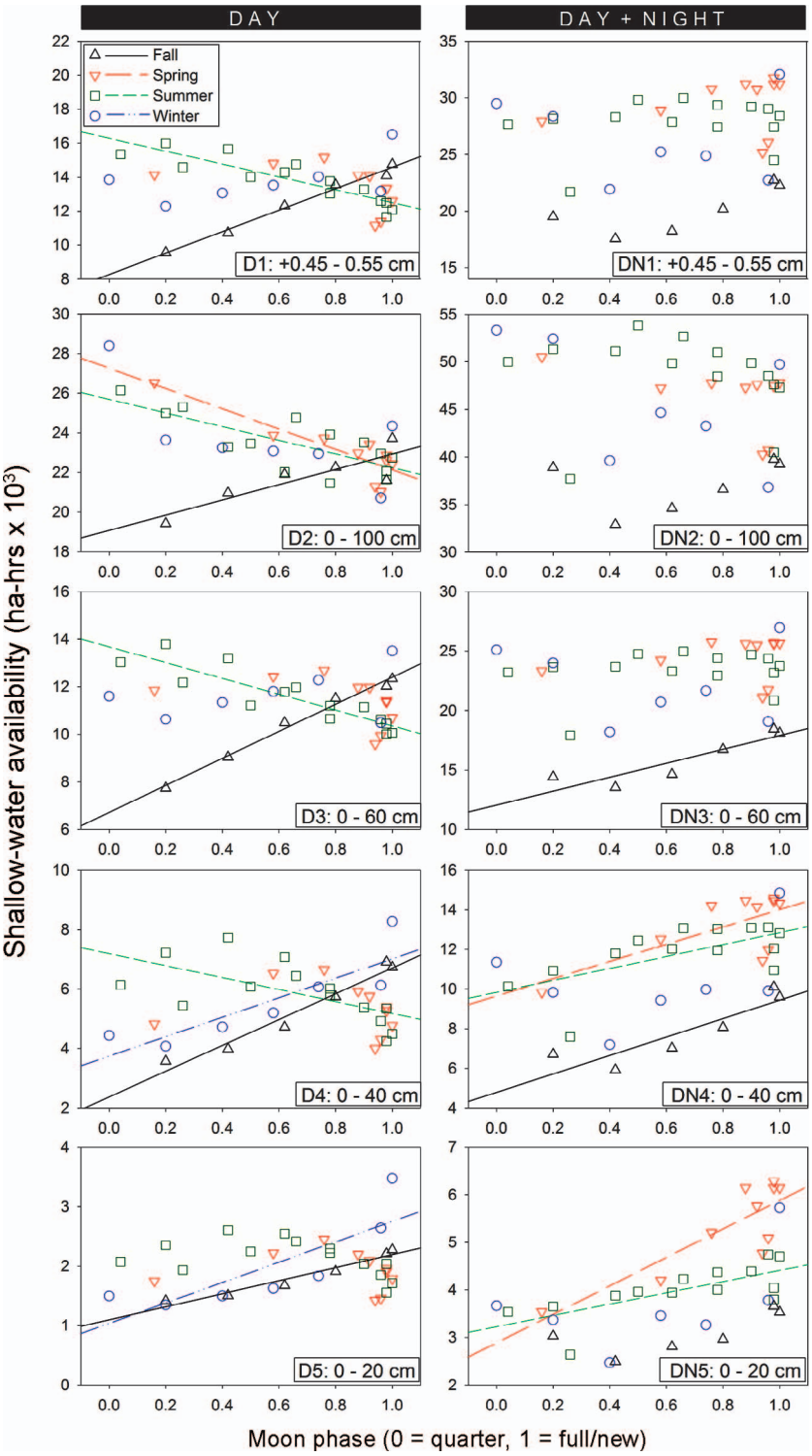

FIGURE 3. Shallow-water Availability versus Moon Phase for Daytime-only and Day plus Nighttime tides, across a range of water depths. D1 corresponds to the water-depth range and the time constraint applied to model the diurnal shallow-water availability for Little Blue Herons, whereas D2 corresponds to the water-depth range for Great White Herons. Linear regressions are only presented when significant at 0.05 alpha.

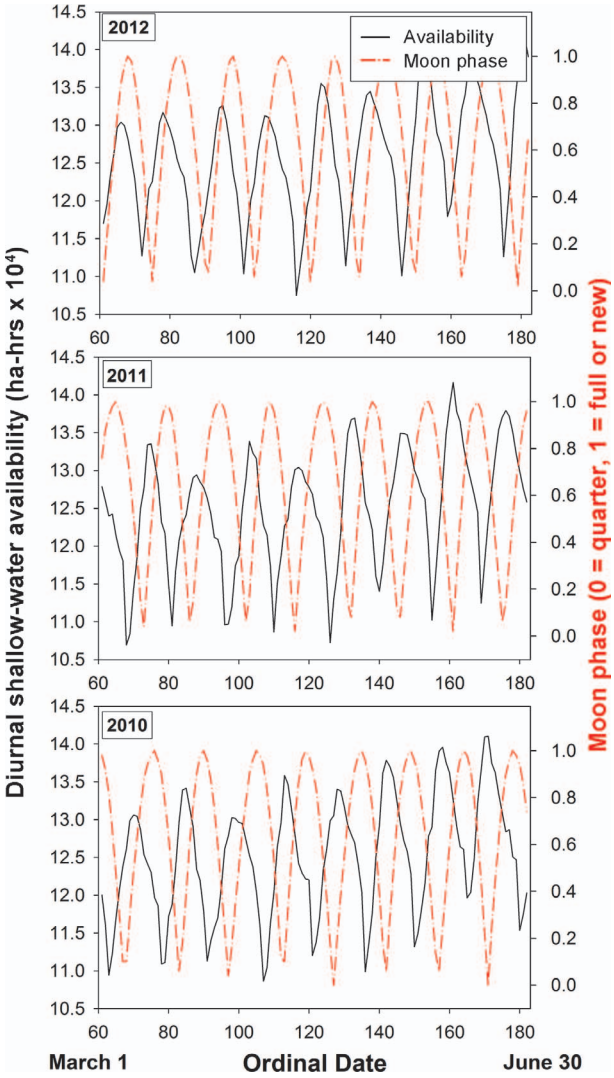

FIGURE 4. Diurnal Shallow-water Availability and Moon Phase for all days between March and June (ordinal dates 61–182) for years 2010–2012.

during a tidal cycle; these were the estimates of shallow-water availability that were used in subsequent analyses. The species-specific water depths were determined from Little Blue Herons ($n = 190$) and Great White Herons ($n = 163$) that were located in space using the method of spot-mapping (Emlin 1977) and collocated onto water depth maps modeled by the TiMSA. The spot-mapped birds were detected during the distribution surveys, among all seasons, and across the full study area. The 10–90% quartile for water depths used by Little Blue Herons (–0.55 m, 0.45 m), values relative to water surface, is a larger range than its leg length (22 cm) would imply, but accounts for TiMSA-modeled error; the water depth range for the Great White Heron was –1.02 m, –0.04 m. An independent evaluation of the TiMSA model (Appendix) demonstrated suitable estimates of water depth for our purposes of determining the availability of shallow water for foraging birds (Figures 8–12).

The Moon Phase as a proxy for the Spring–Neap Tidal Cycle. The TiMSA estimates shallow-water availability, but it did not explicitly track cyclic patterns. Moon Phase was a proxy variable used to track biweekly changes in tidal amplitude (spring–neap tide cycle). The percent illumination of the moon, as documented by the United States Naval Observatory at midnight, was standardized using Equation 1 to allow quarter moons (50% illumination) to correspond to values of 0 (neap tides) and full or new moons (100% or 0% illumination, respectively) to correspond to values of 1 (spring tides); both full and new moons result in similar effects on tidal amplitude.

$$|\text{MoonIllumination} - 0.50|/0.50 \qquad (1)$$

We expected that the abundance of foraging birds would be greatest during full or new moons and lowest during quarter moons, corresponding to spring and neap tides, respectively.

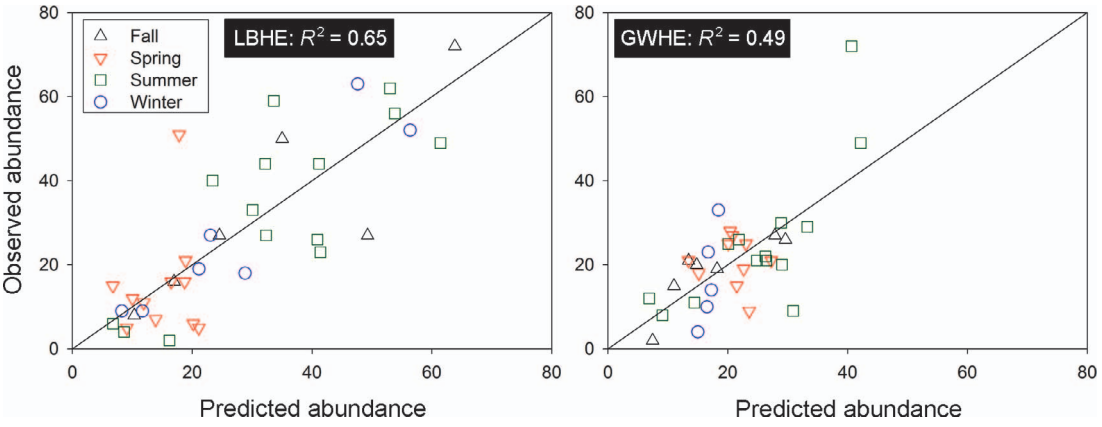

FIGURE 5. The abundance of foraging Little Blue Herons (LBHE, $n = 38$) and Great White Herons (GWHE, $n = 35$) as explained by a model that predicts the abundance of foraging birds. The top model from the model selection analysis was used for prediction.

TABLE 2. Results from model selection analysis for models predicting the abundance of foraging Little Blue Herons. Listed below are the number of parameters in a model (k), the difference in AIC_c between a model and the top model (ΔAIC_c), and the weight of evidence (w_i) as a percentage of (w_i) from all models. The parameter estimates for the top model are also listed below, along with data range for each variable (Data [min, max]), and Abundance Multipliers, which are the fold-change in the number of predicted birds.

Model	Log-likelihood	AIC_c	k	ΔAIC_c	w_i
MoonPhase + ShallowWaterAvailability + TimeFromSunrise + TimeFromLowTide + [Spring,Winter]	−187.67	391.32	8	0	0.82
MoonPhase + ShallowWaterAvailability + TimeFromSunrise + Spring	−190.94	395.89	7	4.55	0.08

Parameter	Estimate	SE	95% CI	Data [min,max]	Abundance Multiplier [low, high]
Intercept*	0.9185	0.2189	[0.4895, 1.3475]		2.51
MoonPhase*	1.8068	0.1548	[1.5034, 2.1102]	[0, 1]	[1.00, 6.09]
ShallowWaterAvailability*	0.0007	0.0001	[0.0005, 0.0009]	[42, 2514]	[1.03, 5.81]
TimeFromLowTide * (ebb/flood tide)	0.0018	0.0007	[0.0004, 0.0032]	[−220, 71]	[0.67, 1.14]
TimeFromSunrise* (time of day)	0.0016	0.0002	[0.0012, 0.0020]	[46, 792]	[1.08, 3.55]
Season[Spring]*	−0.6615	0.1091	[−0.8753, −0.4477]	{0,1}	0.52
Season[Summer]*	0.2498	0.1014	[0.0511, 0.4485]	{0,1}	1.28
Season[Winter]	0.0537	0.1104	[−0.1627, 0.2701]	{0,1}	NA

Season[Fall], not shown, is the baseline season from which abundances in other seasons are compared.
* 95% confidence intervals do not overlap zero and are statistically significant variables.

Season. Seasonal changes in abundance of wading birds are known to result from seasonal dispersal outside of the Keys, or a shift to foraging areas outside our study area that might be closer to distant nesting colonies (e.g., Custer and Osborn 1978, Smith 1995). Although not of primary interest in our study, we felt it necessary to account for seasonal changes in abundance. In our analysis, Season (Winter, Spring, Summer, Fall) was treated as a categorical variable, indicating the season in which the survey was conducted.

Statistical Analyses

We tested our first hypothesis, that shallow-water availability and spring–neap tidal cycles would be strongly correlated (positive for spring-tides and negative for neap-tides) using linear regression models that predicted shallow-water availability from moon phase for each season. For this purpose, we compiled TiMSA estimates of shallow-water availability for daytime-only and daytime plus nighttime time periods, along with estimates of the moon phase, for each survey day. We also included shallow-water availability estimates for a set of increasing water-depth ranges to address potential nonlinear effects due to the water depth that may influence the relationship. For all tests of statistical significance, alpha was fixed a priori at 0.05, and a Student's t-test was applied to test if the parameter estimates significantly differed from zero. In addition to survey-specific analyses, we obtained estimates of daytime shallow-water availability and moon phase for every day from March through June for 3 years (2010–2012) to evaluate the phase between shallow-water availability and moon phase for a biologically relevant timeframe (i.e. breeding period), independent of our survey dates. The wave properties (phase difference and coherence) of shallow-water availability and moon phase were assessed visually.

A model selection approach (Burnham and Anderson 2002) was used to evaluate models predicting the abundance of foraging birds, with an ultimate goal to evaluate hypotheses II–V, which were not mutually exclusive. Furthermore, with the exception of Season (included in all models), all variables were considered independently and in combination. An interaction term was only considered for the effect of Moon Phase and Season. Models were analyzed as Poisson-distributed counts (log-link function) in a generalized linear model framework. Partial residual plots confirmed the linearity assumption for the variables in the models. A correlation matrix and variance inflation factors (VIF) were used to evaluate colinearity among the model variables before analysis (Zar 1999; Table 2). Although moderate correlation ($r < 0.63$) existed between some of the variables, the VIFs were all less than 3, suggesting that multi-colinearity was not an issue and the parameter estimates (mean, SE) could be interpreted without concern. Support for a model was based on Akaike's Information Criterion (AIC) with correction for small sample sizes (AIC_c; Burnham and Anderson 2002). Parameter estimates were considered

statistically significant if their 95% confidence intervals did not overlap zero (Burnham and Anderson 2002). All statistical analyses were performed using statistical software R version 3.0.1 (R Development Core Team 2008).

RESULTS

Hypothesis I: Shallow-Water Availability and Spring–Neap Tidal Cycles

For Little Blue Herons, the sign of the correlation between shallow-water availability and moon phase differed by season, but the direction of the correlation did not change sign among water-depth ranges within a season (Figure 3). For Great White Herons, the relationship between shallow-water availability and moon phase was positive or nonsignificant for each season (Figure 3). The water depth range used to estimate shallow-water availability also appeared to have affected the presence of a significant correlation (Figure 3), although disentangling the reasons behind these differences was problematic due to highly nonlinear effects between the bathymetry and the temporal dynamics of the water surface.

The second modeling study provided simulated data, across a longer and more continuous timeframe, which gave insight into the inconsistent relationship between moon phase and daytime-only shallow-water availability among seasons. Within a single year, the phase difference between daytime-only shallow-water availability and moon phase shifted in-phase (i.e. matching peaks and troughs) and out-of-phase (i.e. opposing peaks and troughs) across the dates modeled (Figure 4). The magnitude of the phase difference (i.e. difference in days between peaks or troughs among the 2 waves) in the early part of March (ordinal dates 61–92) was less in 2012 than in 2011 or 2010 (Figure 4). The change in phase difference over time affected the sign and strength of the correlation between diurnal shallow-water availability and moon phase, which indicates that diurnal shallow-water availability is influenced to a greater extent by the daytime tidal height than by biweekly changes in tidal amplitude. The inconsistent relationship in our study area between moon phase and daytime-only shallow-water availability was a product of the unequal tide heights between 2 consecutive low tides and the daily phase-shift in the time of tide (Figure 1), effectively decoupling the biweekly change in tidal amplitude with diurnal changes in shallow-water availability.

Model Selection Results

The top model predicting Little Blue Heron abundance included the additive effects of Moon Phase, Shallow-water Availability, TimeFromSunrise, TimeFromLowTide, and seasonal effects of Spring and Winter (weight of evidence, $w_i = 0.91$; Table 2). The second and only other model within 10 AIC_c from the top model had terms for Moon Phase, Shallow-water Availability, TimeFromSunrise, and a seasonal effect of Spring ($w_i = 0.09$). A significant positive effect of the variable TimeFromLowTide indicated a marginal effect due to survey, or that abundance increased with the flooding tide, but it is not clear which was the case. Moon Phase was the most important variable (by magnitude of effect) in explaining the variation in the abundance of foraging Little Blue Herons (Table 2), whereas it was the second most important variable for Great White Herons (Table 3). The effect of Moon Phase on the abundance of foraging Little Blue Herons was positive and equal in magnitude across all seasons, ranging between a 0-fold change in abundance during neap tides to a 6.09-fold change in abundance during full or new moons (Table 2). The top model for predicting the abundance of foraging Little Blue Herons had an $R^2 = 0.65$ (Figure 5).

For Great White Herons, there was strong support for one model ($w_i = 0.99$; Table 3), which included effects of Moon Phase, Shallow-water Availability, TimeFromSunrise, seasonal effects of Spring and Winter, and 2 interaction terms between Moon Phase and Spring/Winter. The interaction term effectively changed the magnitude of effects by Moon Phase and the seasonal effects of Spring/Winter. For Great White Herons in Spring, the top model predicted an abundance multiplier from the effect of Moon Phase in the range of a 0.85-fold decrease in abundance during neap tides and a 4-fold increase in abundance during spring tides (Table 3). Similarly in Winter, the top model predicted an abundance multiplier from the effect of Moon Phase in the range of a 0.61-fold decrease in abundance during neap tides and a 3-fold increase in abundance during spring tides (Table 3). The top model for predicting the abundance of foraging Great White Herons had an $R^2 = 0.49$ (Figure 5).

Hypotheses II–V were evaluated based on the parameter estimates in the model selection analysis. There was support for the hypothesis that shallow-water availability is positively correlated with bird abundance for both species (Hypothesis II). Contrary to expectations from Hypothesis III, we found that Moon Phase had a positive effect on the abundance of Little Blue Herons at similar magnitude of effect on abundance as daily changes in diurnal shallow-water availability. Finally, we found no support that the abundance of foraging Little Blue Herons would decline later in the day (Hypothesis IV), or that time of day would not be a significant factor in predicting abundance of foraging Great White Herons (Hypothesis V). In fact, foraging abundance of both species was greatest later in the day (Tables 2 and 3).

DISCUSSION

Daily Tidal Schedules: Constraints on Foraging Time of Diurnal Feeders

The difference in explanatory power between the predictive models of foraging abundance for both study species

TABLE 3. Results from model selection analysis for models predicting the abundance of foraging Great White Herons. See Table 2 legend for details.

Model	Log-likelihood	AIC_c	*k*	ΔAIC_c	w_i
MoonPhase + ShallowWaterAvailability + TimeFromSunrise + [Spring,Winter] + MoonPhase:[Spring,Winter]	−141.07	302.15	10	0	0.99

Parameter	Estimate	SE	95% CI	Data [min,max]	Abundance Multiplier [low, high]
Intercept*	0.7964	0.3586	[0.0935, 1.4993]		2.22
MoonPhase*	1.5897	0.4067	[0.7926, 2.3868]	[0, 1]	[1.00, 4.90]
ShallowWaterAvailability*	0.0003	0.0001	[0.0001, 0.0005]	[42, 2514]	[1.03, 5.29]
TimeFromSunrise* (time of day)	0.0011	0.0002	[0.0007, 0.0015]	[46, 792]	[0.77, 1.09]
Season[Spring]*	1.2053	0.3833	[0.4530, 1.9566]	{0,1}	3.34
Season[Summer]	0.4142	0.3727	[−0.3163, 1.1447]	{0,1}	NA
Season[Winter]*	1.0954	0.3869	[0.3371, 1.8537]	{0,1}	3.33
MoonPhase:Spring*	−1.3587	0.4647	[−2.2695, −0.4479]	[0, 1]	[0.85, 4.21]
MoonPhase:Summer	0.0633	0.4652	[−0.8485, 0.9751]	[0, 1]	NA
MoonPhase:Winter*	−1.5912	0.5810	[−2.7300, −0.4524]	[0, 1]	[0.61, 2.99]

Season[Fall], not shown, is the baseline season from which abundances in other seasons are compared.
* 95% confidence intervals do not overlap zero and are significant variables.

suggest that changes in the daily schedules of tidal flooding, relative to light–dark cycles, places more severe constraints on the feeding time of the shorter-legged, daytime-feeding Little Blue Heron than on the Great White Heron. Of particular importance here is the relative influence of the daily time-shift in the tides on the magnitude of diurnal shallow-water availability. During some seasons in our study, we found a negative correlation between diurnal shallow-water availability and spring tides, contrary to intuition, but due to the time-shift of low tides with unequal tide heights. In a mixed semi-diurnal tidal system, the time-shift in the tide influences the tide height to a greater extent than biweekly changes in tidal amplitude, which is masked by the larger differences in tide height between 2 consecutive low tides.

The strong predictive power of daily tidal schedules on abundance patterns of foraging Little Blue Herons also suggest that any factors affecting nighttime foraging conditions (e.g., nighttime tide height, moon illumination, predation risk) do not substantially affect the daytime abundance of foraging Little Blue Herons. Great White Herons actively forage at night (Powell 1987), which may explain patterns in daytime abundance not captured in our study (Robert et al. 1989). Most of the evidence from the literature points to daytime foraging by Great Blue Herons being complementary to daytime feeding, as opposed to a preferential behavior for fulfilling energetic requirements (Black and Collopy 1982, McNeil et al. 1993, Martin and Raim 2014), but it is unclear to what extent day versus nighttime foraging habits are exhibited in our study area.

Biweekly Changes in the Abundance of Foraging Birds: A Link across Trophic Levels?

Daily tidal cycles make shallow water widely available to foraging wading birds and are established drivers of foraging bird abundance (Powell 1987, Granadeiro et al. 2006, Raposa et al. 2009), which was also apparent in our study. However, biweekly changes in tidal amplitude are rarely examined in studies of wading birds in intertidal environments (but see Matsunaga 2000), nor are their relative effects evaluated against more proximate factors such as daily tidal cycles. To our knowledge, we provide the first evidence that the effect on abundance from daily changes in shallow-water availability is similar in magnitude to the effect from moon phase and the response to moon phase cannot be explained by changes to foraging habitat availability during spring–neap tidal cycles.

For many marine species, synchronous behavior (i.e. numerical response in abundance) with spring–neap tidal cycles can be viewed as advantageous (Takemura et al. 2010) if the spring–neap tidal cycle is also associated with survival benefits such as changes in access to important shallow-water feeding locations or changes in prey availability (Matsunaga 2000). If the biweekly cyclic pattern in the abundance of foraging wading birds is not directly due to lunar-driven physical changes to their shallow-water feeding habitat, then it is plausible that the biweekly cyclic pattern in bird abundance may instead be due to changes in their prey's ecology, as a function of lunar-driven physical changes (e.g., tide height, tidal

current) in the environment. A strong patterning to cyclical changes in prey availability provides an alternative explanation for our findings.

There is already some evidence for the movement and aggregation of aquatic fauna (many of which may be suitable wading bird prey) to occur in strong association with various tidal periodicities driven by the moon phase. However, many aquatic fauna differ in their response to lunar-driven changes in the environment. Some species increase their activity and abundance during quarter moons (neap tides; Morgan 1996, Acosta et al. 1997), whereas other species respond more strongly to new or full moons (spring tides; Lowerre-Barbieri 1998). Other species respond only to the degree of illumination as a cue to biweekly tidal cycles (Hedd et al. 2001, Benoit-Bird et al. 2009, Lea et al. 2010) and there is evidence of physiologically mediated responses to the moon phase (Takemura et al. 2010). The variability in behavioral responses of aquatic fauna to the moon phase should serve as an impetus for targeted studies regarding the relationship between wading birds, their prey, and the moon phase. Such studies may provide evidence for, or against, more direct trophic linkages to external physical forces such as the lunar cycle.

Time of the Tide: Evidence of Effects from Tidal Lags in the Landscape?

Contrary to our expectations, the abundance of foraging wading birds, of both species, increased later in the day. With the exception of actively nesting birds, which may have to feed continuously throughout the day to support nestlings regardless of their individual satiation, such foraging behavior would imply that wading birds are not becoming satiated after foraging early in the day. Our hypothesis did not consider the movement of foraging birds throughout the landscape, a landscape that exhibits large temporal lags in tides between distant locations (up to 3 hr). An increase in wading bird abundance later in the day, as evidenced from our study, may suggest that foraging birds make use of multiple locations in the landscape as shallow-water habitat becomes available, but converge upon the remaining available foraging habitat by day's end. Similar tide-tracking behavior at the landscape scale has been documented in other wading birds (Burger et al. 1977, Raposa et al. 2009). Studies of Grey Herons (*Ardea cinerea*) foraging in intertidal zones also documented limitations in the amount of time that prey (Regós 2011) and shallow water (Lekuona 1999, Matsunaga 2000) are available during tides and as a consequence of tidal lags. Similar findings were reported by Powell (1987) for Great White Herons. Together, this evidence suggests that the spatiotemporal availability of prey and/or water depth is sometimes a limiting factor for foraging wading birds, which has already been demonstrated as having important ecological significance to aquatic species that rely on tides to access habitat for various needs (Gibson et al. 1996, Gibson 2003). Tidal lags within the landscape matrix may also provide multiple areas for marine fauna to fulfill their survival requirements and, therefore, the spatiotemporal matrix of habitats may be more important than previously considered in coastal ecology (Boström et al. 2011).

Diurnal Shallow-Water Availability and Biweekly Tides: Implications for Survey Design

For mixed semi-diurnal tidal systems, the relationship between diurnal shallow-water availability and moon phase is not unique to a locality, season, or year, but due to out-of-phase cycles between spring–neap tides and the phase-shift cycle in the time of the tide. The mechanism underlying the changing relationship between diurnal shallow-water availability and moon phase is due to the length of time it takes for one of the (unequal) low tides to shift in time by 12 hr (one cycle ~14.4 days), for example, from 1900 hours (nighttime) to 0700 hours (daytime), which is slightly faster than the time for one spring–neap tide cycle (~14.75 days). The impact of the differences in wave speed is such that the relationship between diurnal shallow-water availability and moon phase changes continuously, as conceptualized in Figure 1. This realization can have a significant impact on sampling design and interpretation of data from surveys conducted in intertidal areas (see recommendations by Dias et al. 2006). For example, analyses that are conducted within seasons, or constrained to a single year, may incorrectly interpret effect sizes from environmental variables or assume that interactions between variables are accurately represented. In survey design, it is therefore necessary to recognize the wave properties of cyclic environmental variables to ensure that sampling is conducted across time periods where such variables may be in-phase or out-of-phase so as to prevent the misinterpretation of coincidentally correlated variables in short time periods.

TiMSA for Studies of Intertidal Dynamics across Trophic Levels

The tidal model (TiMSA) was successfully applied in this study to evaluate the effects of nonlinear tidal dynamics on shallow-water availability for wading birds that utilized shallow water for feeding. However, the TiMSA may also be used to study the relative effects of tides and other factors on other intertidal migrants. In previous studies, the influence of tides on ecological phenomena has been commonly analyzed by means of mathematical models containing predictor variables such as tide height (reference-point water levels; Powell 1987, Spear et al. 1999, Ellis and Bell 2008, Raposa et al. 2009), tidal flows (ebbing versus flooding tide; Knieb and Wagner 1994,

Matsunaga 2000, Forward and Tankersley 2001), inundation regimes (Rozas and Minello 1998), and moon phase (Spear et al. 1999, Pinet et al. 2011, Reis-Filho et al. 2011). However, these metrics are not dynamic and do not appropriately capture spatiotemporal changes in shallow-water availability, which we have addressed in this study as influential to species' survival requirements (e.g., refuge for predators, access to spawning habitat, fulfillment of energetic requirements). Therefore some of the nuances regarding the impact of tidal dynamics on ecological phenomena may be overlooked. The TiMSA, both as a conceptual framework and as a predictive model, provides a means to assess changes not only to shallow-water availability, but also to habitat, community structure and ecosystem functioning as they relate to tidal fluctuations.

Conclusions

We found that diurnal shallow-water availability was not consistently correlated (in magnitude or direction) with spring–neap tidal cycles, and that the time-shift in the time of the tide impacts diurnal shallow-water availability greater than biweekly changes in tidal amplitude. We find evidence to suggest that changes in abundance associated with spring–neap tidal cycles occur through mechanisms other than changes to shallow-water availability alone. We hypothesize that the underlying mechanism in the observed relationship between the abundance of foraging birds and the spring–neap tidal cycle is through changes in the availability of prey (i.e. changes in prey density or prey vulnerability to capture) that is closely tied to spring–neap tidal cycle itself.

ACKNOWLEDGMENTS

We are grateful for the biological insight and guidance provided by Phillip Hughes and Tom Wilmers. We would like to thank the many volunteers and lab members from the Avian Ecology Laboratory at Florida Atlantic University (FAU) who contributed many field hours and to Michelle Petersen (FAU) who made helpful editorial comments on this manuscript.

Funding: This study was financially supported by U.S. Fish and Wildlife Service awards #40181AG098 and #F12AC01244. None of the funders had any influence on the content of the submitted or published manuscript. None of the funders require approval of the final manuscript to be published.

Ethics statement: Only observations of birds were made, at a distance of 50–500 m, with no perceived disturbance to foraging birds.

Author contributions: LC, DEG, ZX conceived the ideas. LC and LG collected field data. LC developed the TiMSA model. All authors contributed in interpreting the findings and editing the manuscript.

LITERATURE CITED

Acosta, C., T. Matthews, and M. Butler IV (1997). Temporal patterns and transport processes in recruitment of spiny lobster (*Panulirus argus*) postlarvae to south Florida. Marine Biology 129:79–85.

Benoit-Bird, K. J., W. W. L. Au, and D. W. Wisdom (2009). Nocturnal light and lunar cycle effects on diel migration of micronekton. Limnology and Oceanography 54:1789–1800.

Black, B. B., and M. W. Collopy (1982). Nocturnal activity of Great Blue Herons in a north Florida salt marsh. Journal of Field Ornithology 53:403–406.

Boström, C., S. J. Pittman, C. Simenstad, and R. T. Kneib (2011). Seascape ecology of coastal biogenic habitats: Advances, gaps, and challenges. Marine Ecology Progress Series 427: 191–217.

Burger, J., M. A. Howe, D. C. Hahn, and J. Chase (1977). Effects of tide cycles on habitat selection and habitat partitioning by migrating shorebirds. The Auk 94:743–758.

Burnham, K. P., and D. R. Anderson (2002). Model Selection and Multimodel Inference: A Practical Information-Theoretic Approach. Springer Verlag, New York, NY, USA.

Cartwright, D. E., and P. Melchior (1999). Tides: A Scientific History. Cambridge University Press, Cambridge, UK.

Custer, T. W., and R. G. Osborn (1978). Feeding habitat use by colonially-breeding herons, egrets, and ibises in North Carolina. The Auk 95:733–743.

Dias, M. P., J. P. Granadeiro, R. C. Martins, and J. M. Palmeirim (2006). Estimating the use of tidal flats by waders: Inaccuracies due to the response of birds to the tidal cycle: Capsule low tide counts may give inaccurate estimates of habitat use; combining low and mid-tide counts yields better estimates. Bird Study 53:32–38.

Dugan, P. J. (1981). The importance of nocturnal foraging in shorebirds: A consequence of increased invertebrate prey activity. In Feeding and Survival Strategies of Estuarine Organisms (N. V. Jones and W. J. Wolff, Editors). Plenum Press, New York, NY, USA. pp. 251–260.

Emlen, J. T. (1977). Estimating breeding season bird densities from transect counts. The Auk 94:455–468.

Ellis, W. L., and S. S. Bell (2008). Tidal influence on a fringing mangrove intertidal fish community as observed by in situ video recording: Implications for studies of tidally migrating nekton. Marine Ecology Progress Series 370:207–219.

Erwin, R. M (1996). Dependence of waterbirds and shorebirds on shallow-water habitats in the mid-Atlantic coastal region: An ecological profile and management recommendations. Estuaries and Coasts 19:213–219.

Forward, R. B., and R. A. Tankersley (2001). Selective tidal-stream transport of marine animals. In Oceanography and Marine Biology, Volume 39 (R. B. Gibson, M. Barnes, and R. J. A. Atkinson, Editors). Taylor & Francis, New York, NY, USA. pp. 305–353.

Gawlik, D. E (2002). The effects of prey availability on the numerical response of wading birds. Ecological Monographs 72:329–346.

Gibson, R., L. Robb, M. Burrows, and A. Ansell (1996). Tidal, diel and longer term changes in the distribution of fishes on a Scottish sandy beach. Marine Ecology Progress Series 130:1–17.

Gibson, R., L. Robb, H. Wennhage, and M. T. Burrows (2002). Ontogenetic changes in depth distribution of juvenile flatfishes in relation to predation risk and temperature on a shallow-water nursery ground. Marine Ecology Progress Series 220:233–244.

Gibson, R (2003). Go with the flow: Tidal migration in marine animals. Hydrobiologia 503:153–161.

Gill, S. K., and J. R. Schultz (Editors) (2001). Tidal datums and their applications. NOAA Special Publication NOS CO-OPS 1. U.S. Department of Commerce, Silver Spring, MD, USA.

Granadeiro, J. P., M. P. Dias, R. C. Martins, and J. M. Palmeirim (2006). Variation in numbers and behaviour of waders during the tidal cycle: Implications for the use of estuarine sediment flats. Acta Oecologica 29:293–300.

Grothe, P. R., L. A. Taylor, B. W. Eakins, K. S. Carignan, D. Z. Friday, E. Lim, and M. R. Love (2011). Digital Elevation Models of Key West, Florida: Procedures, Data Sources and Analysis. NOAA National Geophysical Data Center technical report. Boulder, CO, USA.

Hedd, A., R. Gales, and N. Brothers (2001). Foraging strategies of shy albatross *Thalassarche cauta* breeding at Albatross Island, Tasmania, Australia. Marine Ecology Progress Series 224:267–282.

Kneib, R., and S. Wagner (1994). Nekton use of vegetated marsh habitats at different stages of tidal inundation. Marine Ecology Progress Series 106:227–238.

Kronfeld-Schor, N., and T. Dayan (2003). Partitioning of time as an ecological resource. Annual Review of Ecology, Evolution, and Systematics 34:153–181.

Lea, M.-A., D. Johnson, S. Melin, R. Ream, and T. Gelatt (2010). Diving ontogeny and lunar responses in a highly migratory mammal, the northern fur seal *Callorhinus ursinus*. Marine Ecology Progress Series 419:233–247.

Lekuona, J (1999). Food and foraging activity of Grey Herons, *Ardea cinerea*, in a coastal area during the breeding season. Folia Zoologica 48:123–130.

Lowerre-Barbieri, S. K., J. M. Lowerre, and L. R. Barbieri (1998). Multiple spawning and the dynamics of fish populations: Inferences from an individual-based simulation model. Canadian Journal of Fisheries and Aquatic Sciences 55: 2244–2254.

Martin, K. L. M., and J. G. Raim (2014). Avian predators target nocturnal runs of the beach-spawning marine fish, California grunion, *Leuresthes tenus* (Atherinoppsidae). Bulletin of the Southern California Academy of Sciences 113:187–199.

Matsunaga, K. (2000). Effects of tidal cycle on the feeding activity and behavior of Grey Herons in a tidal flat in Notsuke Bay, northern Japan. Waterbirds 23:226–235.

McNeil, R., R. Benoit, and J. Desgranges (1993). Daytime and nighttime activity at a breeding colony of Great Blue Herons in a nontidal environment. Canadian Journal of Zoology 71: 1075–1078.

Melvin, S. L., D. E. Gawlik, and T. Scharff (1999). Long-term movement patterns for seven species of wading birds. Waterbirds 22:411–416.

Milbert, D. (2002). VDatum transformation tool (New Version 1.05). The GeoCommunity Spatial News. http://spatialnews.geocomm.com/features/vdatum/

Morgan, S. G. (1996). Influence of tidal variation on reproductive timing. Journal of Experimental Marine Biology and Ecology 206:237–251.

Nichols, J. D., J. E. Hines, J. R. Sauer, F. W. Fallon, J. E. Fallon, and P. J. Heglund (2000). A double-observer approach for estimating detection probability and abundance from point counts. The Auk 117:393–408.

Paterson, A. W., and A. K. Whitfield (2000). Do shallow-water habitats function as refugia for juvenile fishes? Estuarine, Coastal and Shelf Science 51:359–364.

Perillo, G. M., E. Wolanski, D. R. Cahoon, and M. M. Brinson (2009). Coastal Wetlands: An Integrated Ecosystem Approach. Elsevier, Amsterdam, The Netherlands.

Pinet, P., A. Jaeger, E. Cordier, G. Potin, and M. Le Corre (2011). Celestial moderation of tropical seabird behavior. PLOS One 6:e27663.

Powell, G. V. N (1987). Habitat use by wading birds in a subtropical estuary: Implications of hydrography. The Auk 104:740–749.

Raposa, K. B., R. A. McKinney, and A. Beaudette (2009). Effects of tide stage on the use of salt marshes by wading birds in Rhode Island. Northeastern Naturalist 16:209–224.

R Development Core Team (2008). R: A language and environment for statistical computing. R Foundation for Statistical Computing, Vienna, Austria. http://www.R-project.org

Regós, A. (2011). Modelling the feeding behavior of Grey Heron (*Ardea cinerea*) in a coastal wetland of NW Iberian peninsula during the wintering season. Animal Biodiversity and Conservation 34:249–256.

Reise, K. (1985). Tidal Flat Ecology: An Experimental Approach to Species Interactions. Springer, Berlin, Germany.

Reis-Filho, J. A., F. Barros, J. D. A. C. D. C. Nunes, C. L. S. Sampaio, and G. B. G. De Souza (2011). Moon and tide effects on fish capture in a tropical tidal flat. Journal of the Marine Biological Association of the United Kingdom 91:735–743.

Rieucau, G., K. M. Boswell, M. E. Kimball, G. Diaz, and D. M. Allen (2015). Tidal and diel variations in abundance and schooling behavior of estuarine fish within an intertidal salt marsh pool. Hydrobiologia 753:149–162.

Robert, M., R. McNeil, and A. Leduc (1989). Conditions and significance of night feeding in shorebirds and other water birds in a tropical lagoon. The Auk 106:94–101.

Rodgers, J. A., Jr., and H. T. Smith (2012). Little Blue Heron (*Egretta caerulea*). In The Birds of North America Online (A. Poole, Editor). Cornell Lab of Ornithology, Ithaca, NY, USA. doi:10.2173/bna.145

Rozas, L. P (1995). Hydroperiod and its influence on nekton use of the salt marsh: A pulsing ecosystem. Estuaries 18:579–590.

Rozas, L. P., and T. J. Minello (1998). Nekton use of salt marsh, seagrass, and nonvegetated habitats in a south Texas (USA) estuary. Bulletin of Marine Science 63:481–501.

Santiago-Quesada, F., S. M. Estrella, J. M. Sánchez-Guzmán, and J. A. Masero (2014). Why water birds forage at night: A test using Black-tailed Godwits *Limosa limosa* during migratory periods. Journal of Avian Biology 45:406–409.

Singh, V. P., and D. K. Frevert (2002a). Mathematical Models of Large Watershed Hydrology. Water Resources Publications, Highlands Ranch, CO, USA.

Singh, V. P., and D. K. Frevert (2002b). Mathematical Models of Small Watershed Hydrology and Applications. Water Resources Publications, Highlands Ranch, CO, USA.
Sitters, H. P., P. M. González, T. Piersma, A. J. Baker, and D. J. Price (2001). Day and night feeding habitat of Red Knots in Patagonia: Profitability versus safety? Journal of Field Ornithology 72:86–95.
Smith, J. P (1995). Foraging flights and habitat use of nesting wading birds (Ciconiiformes) at Lake Okeechobee, Florida. Colonial Waterbirds 18:139–158.
Spear, L. B., S. B. Terrill, C. Lenihan, and P. Delevoryas (1999). Effects of temporal and environmental factors on the probability of detecting California Black Rails. Journal of Field Ornithology 70:465–480.
Takemura, A., M. Rahman, and Y. Park (2010). External and internal controls of lunar-related reproductive rhythms in fishes. Journal of Fish Biology 76:7–26.
Vennesland, R. G., and R. W. Butler (2011). Great Blue Heron (*Ardea herodias*). In The Birds of North America Online (A. Poole, Editor). Cornell Lab of Ornithology, Ithaca, NY, USA. doi:10.2173/bna.25
Verweij, M. C., I. Nagelkerken, S. L. J. Wartenbergh, and I. R. P. G. van der Velde (2006). Caribbean mangroves and seagrass beds as daytime feeding habitat for juvenile French grunts *Haemulon flavolineatum*. Marine Biology 149:1291–1299.
Weisberg, S. B., R. Whalen, and V. A. Lotrich (1981). Tidal and diurnal influence on food consumption of a salt marsh killifish *Fundulus heteroclitus*. Marine Biology 61:243–246.
Yu, Y., and C. Swennen (2004). Feeding of wintering Black-faced Spoonbills in Hong Kong: When and how long? Waterbirds 27:135–140.
Zar, J. H (1999). Biostatistical Analysis. Pearson Education, New Delhi, India.

APPENDIX

A Tidal Inundation Model of Shallow-Water Availability

1. Methods. *1.1.1 Model purpose***.** Tidal fluctuations influence the time that tidal migrants can devote to survival requirements, such as foraging for food. The model was designed to estimate the spatiotemporal availability of a user-defined range of ecologically relevant water depths, thus improving our ability to model ecological relevant behaviors at a spatiotemporal scale representative of real-world scenarios.

The model employs a numerical scheme to estimate the rise and fall of water levels during tides in discrete basins. The basins are not predefined, instead the size and extent of each basin is determined by the availability of data from tidal water gauges. The following description is for a numerical tidal model applicable to any region with sufficient data on tides and a digital model for bathymetry with sufficient accuracy suitable for the application purpose.

*1.1.2 Entities, state variables, and scales***.** The model entities, or independent objects that may interact, are the Theissen Polygons. The model provides a backdrop of environmental change (i.e. defined by the state variables). The model state is defined as spatially explicit grid-cells, each of which is characterized by its availability in time. The time-step of the model is 1 minute. However, the temporal resolution will be limited by the spatial resolution. The spatial resolution of the model grid-cell is defined by the spatial resolution of the underlying DEM. The model grid-cell thus has units of area-time (e.g., ha-hrs). The model's state changes as a result of a discrete, data-driven, numerical tidal fluctuation scheme.

*1.1.3 Process overview and scheduling***.** The model simulates tides using freely available point-data for the height and time at high- and low-tide, obtained from nearby tidal gauges ($N = 37$) networked within the study area (Figure 6). Our model employs Thiessen (Voronoi) polygons, or individual polygons whose boundaries define an area that is closest to each data point, relative to all other data points in the model (Figure 6).

The flow of information for calculating the temporal availability within a particular *water-window* is provided in Figure 7, and its detailed description is as follows. The modeling process commences with duplicate Mean Lower Low Water (MLLW) reference maps; tidal simulation occurs independently for the Ebb and Flood components of the low tide (Figure 7, letter A). The reference map (MLLW map) is adjusted so that the height of sea levels at low tide reflects data for Day (n) (Figure 7, letter B). A tide is simulated by numerically adding water to every grid-cell (Figure 7, letter C). For every minute a grid-cell resides within the foraging *water-window*, 1 minute of foraging time is added to the grid-cell (Figure 7, letter D). This process continues for the duration of the tide and results in a spatially explicit map of shallow-water availability, which displays availability in minutes unconstrained by daylight availability. Diurnal constraints limit calculations of shallow-water availability to the hours between sunrise and sunset, or other user-defined time constraints (Figure 7, letter E). The final map is for one day (Figure 7, letter F). Estimates of shallow-water availability for a grid-cell have units of time. An estimate of shallow-water availability is obtained by multiplying the total temporal availability by its spatial area, giving units of area-time (e.g., ha-hrs).

*1.1.3.1 Temporal availability***.** A) *Rate of change in sea level (ΔSL).* To determine temporal shallow-water availability, we calculated how long an area resides within a *water-window*. The ΔSL follows a dynamic, but predictable, pattern that can be approximated using the sine function. The rate at which sea levels change, and the rate of change of the sine function, have a maximum at the midpoint between high and low tide, and a minimum at exactly high and low tide. Our approximation of sea level change in this way essentially gives greater weight (in time) to areas that are available (within the *water-window*) at low or high tide. The sine function for the approximation of sea

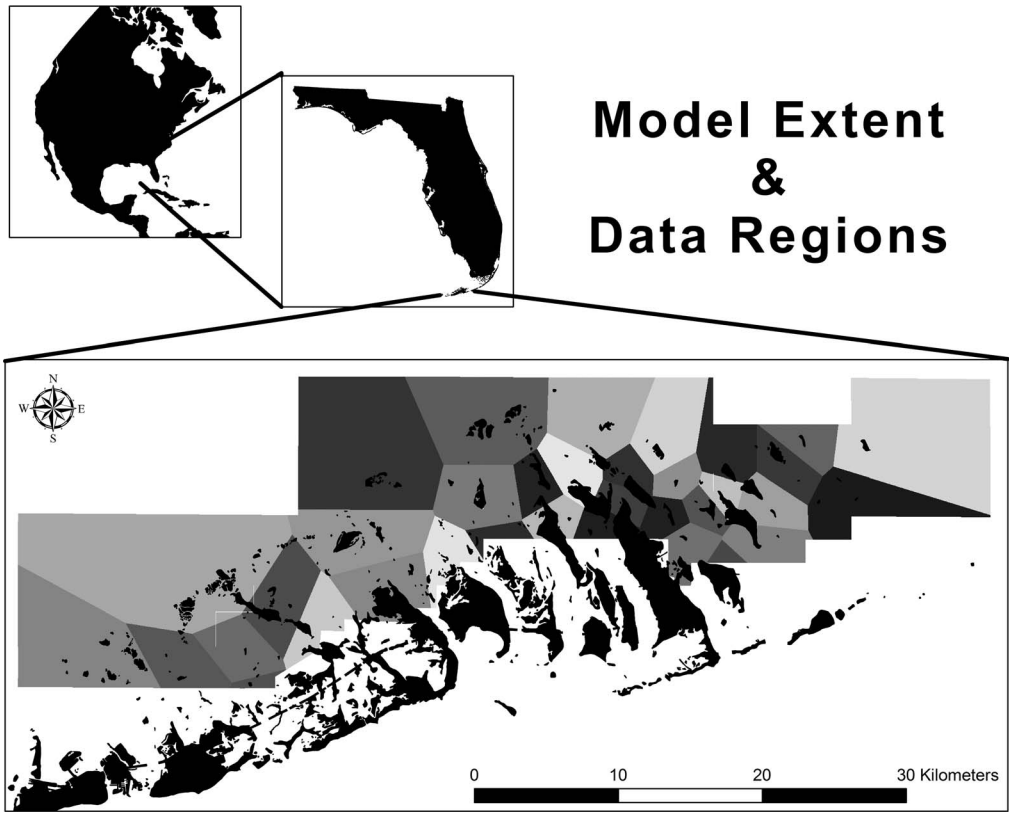

FIGURE 6. A map of the study area, located within the lower Florida Keys archipelago, and the Theissen, or Voronoi, polygons (shaded) used in the modeling process. The polygon boundaries define an area that is closest to a unique tidal gauge (located in the center of each polygon), thus allowing tidal dynamics to differ in amplitude and wave period between polygons.

level change is provided by the following set of equations:

$$Y_t = \frac{TRange}{2} * \sin\left[\left(\frac{\pi}{P} * (p-1)\right) - \left(\frac{\pi}{2}\right)\right] \quad (2)$$

$$Y_{t+1} = \frac{TRange}{2} * \sin\left[\left(\frac{\pi}{P} * p\right) - \left(\frac{\pi}{2}\right)\right] \quad (3)$$

$$\Delta SL = Y_{t+1} - Y_t \quad (4)$$

where ΔSL is the change in sea level, Y is the height of sea level at time *t*, TRange is the tidal range, P is the tidal period, and p is the time within the tidal period for which the height of sea level is predicted.

B) *Half-tide simulation*. Ebb (water going out) and flood (water coming in) tide components have unique tidal dynamics (wave period and amplitude), and tides are characteristically asymmetrical in our study area. For this reason, we conduct the tidal simulation separately for both the ebb and flood components of the tide (hence, "half-tide" simulation). We simulate a half-tide by adding the change in water depth every 1minute to our water depth reference map. For every 1 minute that an area resides within the *water-window* [lower-bound (L), upper-bound (U)], 1 minute is added to that area's estimate of availability (unit = minutes):

$$if\,(L \leq waterdepth \leq U) \quad (5)$$

$$then\{Availability_{t+1} = Availability_t + 1\} \quad (6)$$

1.1.3.2 Diurnal availability for foraging. Little Blue Herons are known to leave their roosts at dawn to forage and abandon foraging at dusk. For our particular study, we restrict available foraging times, and therefore the estimates of shallow-water availability, to the period of time between sunrise and sunset. This constraint could easily be modified to fit unique activity patterns of other species.

1.1.4 Input data. A digital elevation model (DEM), with the vertical datum of mean high water, was obtained for the study area from the NOAA Tsunami Inundation Project (Grothe et al. 2011; Table 1). The DEM has a horizontal resolution of 30 m and an estimated vertical accuracy of 0.10 m in shallow waters or 5% of water depth in deeper waters (Grothe et al. 2011). The DEM was converted from mean high water to the mean lower low water (MLLW) datum using the freely available VDatum transformation tool (Milbert 2002). Tidal data was freely obtained for each tide gauge in the model's domain (Table

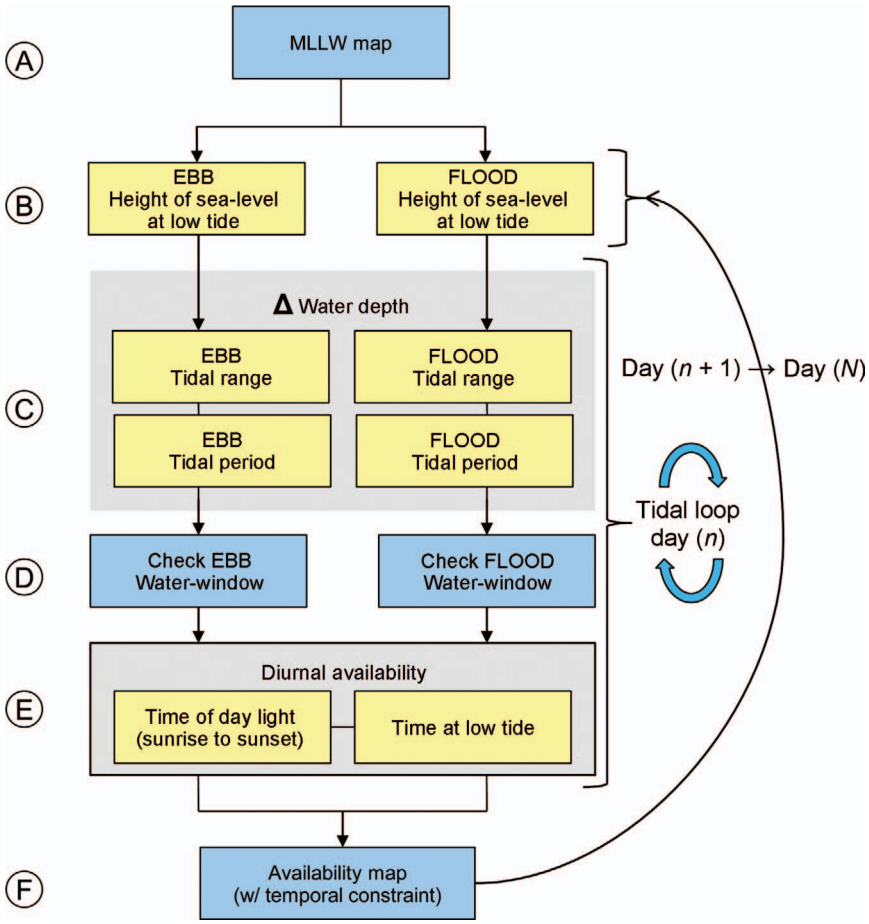

FIGURE 7. A flow chart for modeling shallow-water availability for a diurnally active species. The circled letters correspond to steps in the modeling process. Circled letters on the left of the figure correspond to boxes, as well as arrows, that are immediately to the right. Boxes in blue represent datasets that are in the spatially explicit ASCII format whereas boxes in yellow represent datasets that are in a comma separated value (CSV) format. Details of the modeling process (circles A–F) are provided in the text.

1). Visual Basic for Applications (VBA), in Microsoft Excel 2010, was used to format the data into a comma-separate value, tabular format suitable for simulation.

1.1.5 Model assumptions.

a) Temporal availability of shallow water is a function of (1) the tidal height, (2) the tidal range of the ebb/flood components of a low tide, (3) the rate of change of water levels, and (4) biological time constraints, which for our purposes is limited to the time between sunrise and sunset.
b) The nearest tidal gauge to a cell provides the most accurate information on that cell's (1) time at high/low tide, (2) tidal height at high/low tide, (3) tidal range and tidal period (4) of the ebb/flood components of a low tide.
c) The unit "area-time" is an ecologically relevant unit for shallow-water availability.
d) Wind plays a negligible role in shallow-water availability estimates.
e) The sine function approximates the rate of sea level change for the ebb/flood components of a low tide, and this rate of sea level change is equal within each tidal data region (Thiessen polygon).

1.2 Model Evaluation. *1.2.1 Water depths.* Accurate point estimates of water depth are required to evaluate modeled water depth predictions. We therefore conducted water depth surveys (April 2011) to compare and evaluate the model's ability to predict point-estimates of water depth in space and over time. A stratified random sampling design (by elevation [low, high], spatial scale [5 m, 500 m]) was employed at 14 sampling locations. At each sample location, 5 meter sticks were set into the sediment 5 m apart and their GPS coordinates were recorded (14 sample locations * 5 meter sticks per location = 70; $N = 70$ samples). An observer using binoculars, stationed in an anchored kayak or boat nearby, recorded the time, the actual water depth to the nearest centimeter, and the reference mark.

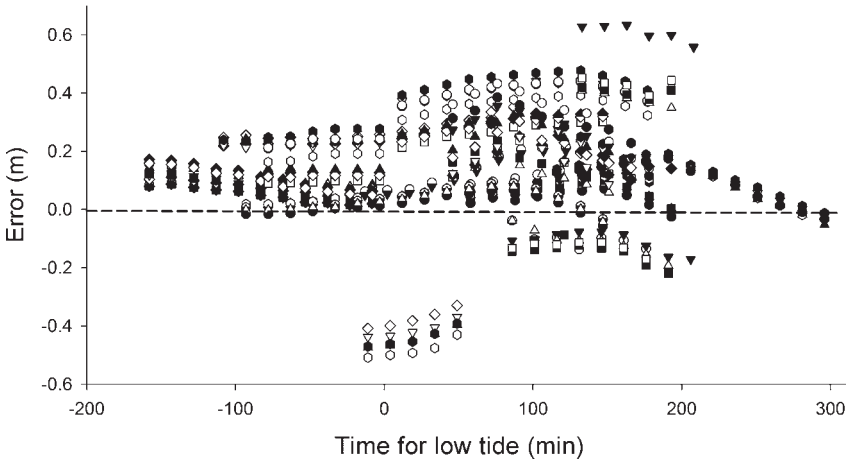

FIGURE 8. Model error (water depths predicted by the TiMSA minus water levels observed) versus time from low tide. The error for each sample ($N = 70$, with repeated measures), represented as unique symbols, is plotted versus the time from low tide, which is obtained from the nearest tidal gauge in the area. The TiMSA consistently predicted greater water depths than those observed, although the absolute error differed significantly between sites. The DEM error is reflected in the absolute difference between predicted water levels and those observed at low tide (e.g., when time from low = 0). Local maximums in model error occur during flood tides (positive values on x-axis), but model error quickly declines thereafter. The change in model error during flood tides may be explained by topographic features (e.g., configuration or contours, distance to a channel) or vegetation that shield the flooding tide, resulting in model-observation mismatch.

We employed a linear mixed effects model in R version 3.0.1 (package "nlme"; R Development Core Team, 2008) to investigate the impact of mean elevation (vertical datum: mean lower low water, ELEV) and distance to the nearest tide gauge (DIST) as possible contributors to the spatial error terms. The fixed effects were DIST, ELEV, and in order to account for repeated measures samples within each sample location ($N = 70$), the random effect time from low tide (TFL) was nested within each sample. We assessed statistical significance at alpha = 0.05. In addition, we graphically evaluated the effect of TFL on the overall error among the samples.

1.2.2 Shallow-water availability. Shallow-water availability, or time within a *water-window,* is expected to have inherent error associated with the point estimates of water depth made by the model. However, it is unclear how estimates made at different temporal periods will be affected by the modeled error and if the results, with error included, will be proportional to what is observed. To understand how our modeled availability estimates varied over time, we used high accuracy (± 0.03 m) water level data loggers (HOBO U-20-Ti; Onset Computer, Bourne, Massachusetts, USA) to obtain water depths at 7 distinct locations in the study area between January and April 2013. Each HOBO data logger recorded water depths for a timeframe of approximately 600 min over the course of a tidal cycle. Locations where the HOBOs were deployed were selected to investigate the effect of distance to the nearest tidal gauge on predicted water depths. The data loggers recorded water depths every 5 minutes surrounding the slack low tide. The HOBO-observed water depth at low tide was used as an error adjustment for DEM (vertical datum: mean lower low water, MLLW). As an example, if the HOBO-observed low tide water depth was recorded as 0.30 m, and the day-adjusted DEM reports an elevation of 0.50 m (MLLW), then the error-adjustment would be applied as {0.30 m − 0.50 m = –0.20 m DEM error}. Inundation times were modeled at each data point with and without the error adjusted DEM. For comparison to observed availability times, availability estimates were modeled by the TiMSA at each HOBO location with and without the error adjusted DEM. Error associated with estimates of availability (inundation times) were evaluated graphically.

1.3 Model Application. *1.3.1 Front-end graphical user interface.* Model flexibility was conceptualized from the beginning of the project, and it was considered to be a requirement that the final model be formalized as a user-friendly front-end product. The C# programming language was used to design the graphical user interface (GUI). Model inputs (e.g., tidal datasets) and temporal outputs (e.g., single tide, days, year) were coded as flexible parameters to be defined by a nontechnical user in the GUI.

Results

2.1 Model Evaluation: Water Depths. Among the 14 sampling locations, the average root mean squared error (RSME) among all sampling locations was 0.21 m ± 0.13 m SD ($n = 14$, range = [0.05 m, 0.43 m]). A ± 20-cm error, as described by the RSME, would certainly require inferences from the model's output to be made with this error in mind.

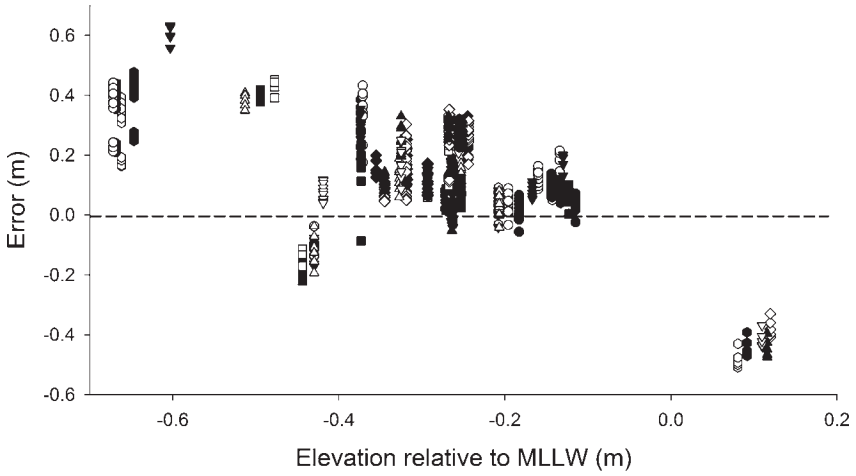

FIGURE 9. Model error versus elevation, relative to mean lower low water (MLLW). The water depths predicted by the TiMSA minus water levels observed constitute the error in the predictions. The error due to tidal simulation can be understood as the vertical spread in a cluster of symbols (sample locations, $n = 70$), while inaccuracies in the digital elevation model (DEM) is evidenced by entire vertical shifts between different symbol clusters (e.g., samples).

The TiMSA does not account for physical processes involved in tidal flow, and as a consequence, the error associated with our predictions tend to rise and fall (Figure 8) as topographic features or attributes of the environment (such as presence/absence of vegetation) effectively shield an ebbing or flooding tidal wave (personal observation); hydrodynamic theory also supports these observations (Singh and Frevert 2002a, 2002b, Perillo et al. 2009). Although we omit the physics of tidal flow in our model, which undoubtedly influences the error in time, we demonstrate that temporal error is minimal when compared to error in the DEM, which overwhelms the error structure:

$$E_{total} = e_{spatial} + e_{temporal} \quad (7)$$

where E is the total prediction error in the model, $e_{spatial}$ is the spatial error resulting from inaccuracies in the DEM, and $e_{temporal}$ is the temporal error due to simplification of tidal dynamics in our model.

When the error structure was investigated further, we found that the average standard deviation of the error at each sampling location ($n = 70$) was 0.05 m (range = [0.02 m, 0.11 m]). The latter error term (average SD) was

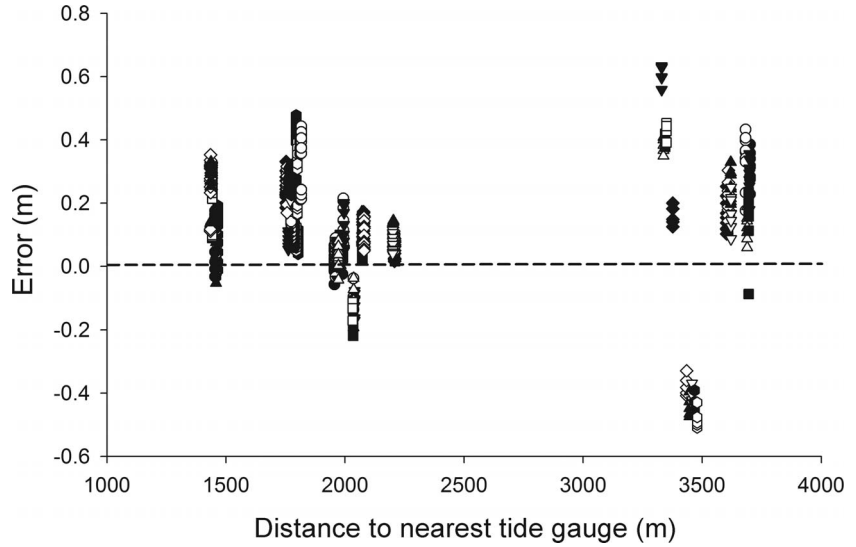

FIGURE 10. Model error versus distance to nearest tide gauge (DIST). The water depths predicted by the TiMSA minus water levels observed constitute the error in the predictions. There was a significant effect of DIST on the total error after controlling for repeated measures sampling in time at each location ($t = -6.006$, df = 699, $p < 0.00$). However, the effect was considerably small, ~0.07-m error for every 1,000 m from the tide gauge.

TABLE 4. Root mean squared error (RMSE) of availability (in minutes) associated with shallow-water categories, as estimated by the TiMSA; actual availability was obtained from HOBO water level loggers. Error-adjusted digital elevation models (DEM-adjusted) reduces the error as predicted by the TiMSA.

Shallow-water Category	RMSE Raw (minutes)	RMSE DEM-adjusted (minutes)
≤ 0.20	59	41
≤ 0.40	71	7
≤ 0.60	108	40
≤ 0.80	66	16
≤ 1.00	64	3

understood as temporal error that stemmed from simplifying the tidal dynamics in space—our use of Thiessen polygons. Absent of spatial error (i.e. error in the DEM; $e_{spatial}$), we would have expected that the total error in the model was primarily due to how we modeled the tides, but this was not what we observed.

We found a significant and inverse relationship between ELEV and the total error ($t = -20.92$, d.f. $= 699$, $p < 0.00$); model error increased as ELEV decreased. The relationship was graphically observed as vertical shifts between samples (Figure 9). There was also a significant effect of DIST on the total error ($t = -6.02$, d.f. $= 699$, $p < 0.00$), also observed as vertical shifts between samples (Figure 10). However, the effect of ELEV on the total error was considerably greater than that of DIST. There was approximately a 0.52 m change in error for every 1 m change in elevation, compared to a 0.07 m change in error for every 1,000 m from the tidal gauge.

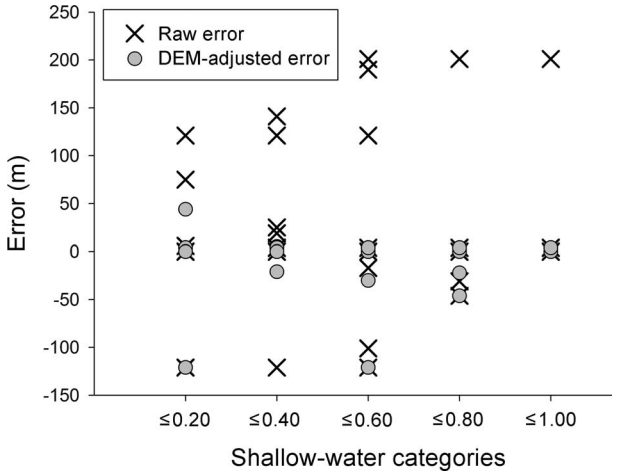

FIGURE 11. Model error associated with estimates of availability (in minutes), plotted across 5 shallow-water categories. The error is defined as estimates of shallow-water availability predicted by the TiMSA minus actual shallow-water availability, as measured by HOBO water level data-loggers ($n = 9$). The error decreases and converges as availability is estimated for larger shallow-water categories. This convergence occurs at lower shallow-water categories when the DEM is error-adjusted (circles).

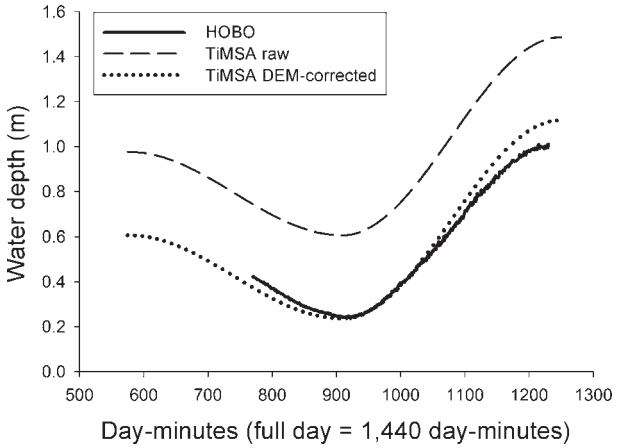

FIGURE 12. TiMSA-predicted water depths (TiMSA Raw) closely match the pattern of observed water depths (HOBO water level data-logger) during tidal fluctuations at a location with an elevation of −1.1 m MLLW and at a distance of ~3 km to the nearest tidal gauge. When the Digital Elevation Model (DEM) is error-corrected (DEM_adjusted), the error between TiMSA predictions and observed water levels is noticeably reduced.

2.2 Model Evaluation: Shallow-Water Availability. Overall, the root mean squared error (RSME) of shallow-water availability predictions ranged from 59 to 108 min (Table 4). Although estimates of shallow-water availability more often matched the observed values (as recorded by HOBO water level loggers) when estimates were made within a larger *water-window* (Figure 11), there was moderate consistency in the RSME among samples in both the Raw and DEM-adjusted TiMSA predictions at all shallow-water categories (Table 4). Moreover, it is expected that estimates made within longer temporal periods (e.g., over a full-tidal cycle) are likely to provide greater distinction in temporal estimates than predictions made within shorter temporal periods (e.g., span of minutes).

From the set of tidal cycles observed ($n = 9$, at 7 distinct locations), the model appears to closely match the observed rise and fall pattern of water levels, albeit with considerable vertical offsets in some samples (Figure 11). However, when the DEM was error-adjusted, the error between predicted and observed water levels was noticeably reduced (Figures 11 and 12); vertical offsets, associated with DEM error, will also directly impact estimates of shallow-water availability. The vertical offsets can be considered mathematical constants, and as such, they can be applied as input into the model to increase the accuracy of shallow-water availability estimates. Nevertheless, these estimates are consistently proportional to reality, which affords us the confidence to use the model's output for studying ecological phenomena.